Testing of a new mixed model for LES: the Leonard model supplemented by a dynamic Smagorinsky term

By G. S. Winckelmans[1], A. A. Wray AND O. V. Vasilyev[2]

A new mixed model which uses the Leonard expansion (truncated to one term) supplemented by a purely dissipative term (dynamic Smagorinsky) has been developed and tested in actual Large Eddy Simulations (LES) of decaying homogeneous turbulence and of channel flow. This model assumes that the LES filter is smooth in wave space, which is the case of most filters defined in physical space (*e.g.*, top hat, Gaussian, discrete filters). The dynamic procedure has been extended for the mixed model. It is used to determine the model coefficient, C, for the added Smagorinsky term. The one-term Leonard model provides significant local backscatter while remaining globally dissipative. In *a priori* testing, its correlation with DNS is greater than 0.9. However, when used on its own in actual LES, this model is found to provide too little dissipation. Hence the need for added dissipation, here provided by the dynamic Smagorinsky term. In 64^3 LES of decaying homogeneous turbulence started from Gaussian filtered 256^3 DNS at $Re_\lambda \simeq 90$, the new mixed dynamic model performs significantly better than the dynamic Smagorinsky model with same Gaussian filtering; it also outperforms the dynamic Smagorinsky model with sharp cutoff filtering: much better energy spectra, much better energy and enstrophy decay. For the preliminary 48^3 LES runs on the channel flow at $Re_\tau = 395$ done with smooth LES filtering (Gaussian in the homogeneous directions, top hat in the non-homogeneous direction), the mixed dynamic model is also superior to the dynamic Smagorinsky model. However, the dynamic Smagorinsky model with sharp cutoff test filtering in the homogeneous directions still produces a better mean velocity profile. This result calls for further investigations.

1. Introduction and model development

We consider incompressible flows ($\partial_i u_i = 0$). Upon applying a spatial filter, $\overline{G}$,

$$\overline{f}(\mathbf{x}) = \int \overline{G}(\mathbf{x}-\mathbf{y})\, f(\mathbf{y})\, d\mathbf{y}\ , \tag{1}$$

to the Navier-Stokes (NS) equations written in the velocity-pressure formulation, one obtains the evolution equation for the filtered velocity field (with $\partial_i \overline{u}_i = 0$):

$$\partial_t \overline{u}_i + \partial_j \left(\overline{u}_i\, \overline{u}_j\right) + \partial_i \overline{P} = \partial_j \left(2\nu\, \overline{S}_{ij}\right) - \partial_j \tau_{ij}\ , \tag{2}$$

1 Mechanical Engineering, Center for Systems Engineering and Applied Mechanics, Université catholique de Louvain, Belgium.

2 Current address: Mechanical and Aerospace Engineering, University of Missouri-Columbia.

with $\overline{P} = \overline{p}/\rho$ the pressure divided by the density, $\overline{S}_{ij} = (\partial_j \overline{u}_i + \partial_i \overline{u}_j)/2$ the symmetric rate of strain tensor, and $\tau_{ij} = \overline{u_i\, u_j} - \overline{u}_i\, \overline{u}_j$ the symmetric stress tensor due to the filtering. This tensor is often called "subgrid-scales" stress tensor. This name is misleading because the filtering above is defined independently of a numerical grid. A better term would be "filtered-scales" stress tensor.

We here consider non-linear models of the family derived from Leonard (1974, 1997). Consider the Gaussian filter, $\overline{\Delta}\,\overline{G}(x) = \exp\left(-x^2/2\overline{\Delta}^2\right)/\sqrt{2\pi}$, $\overline{G}(k) = \exp\left(-k^2\,\overline{\Delta}^2/2\right)$. The Leonard expansion is then obtained as:

$$\overline{f\ g} \simeq \overline{f}\ \overline{g} + \overline{\Delta}^2\, \partial_x \overline{f}\ \partial_x \overline{g} + \frac{\overline{\Delta}^4}{2!}\, \partial_x\partial_x \overline{f}\ \partial_x\partial_x \overline{g} + \frac{\overline{\Delta}^6}{3!}\, \partial_x\partial_x\partial_x \overline{f}\ \partial_x\partial_x\partial_x \overline{g} + \dots \ . \tag{3}$$

This result is remarkable because, at least in principle, it provides a means of evaluating the filter of a product of variables from the filtered variables and their derivatives. In 3-D, the filter is taken as the product of 1-D filters. One then obtains for the stress (Leonard, 1997):

$$\tau_{ij} = \overline{\Delta}^2\, \partial_k \overline{u}_i\, \partial_k \overline{u}_j + \frac{\overline{\Delta}^4}{2!}\, \partial_k\partial_l \overline{u}_i\ \partial_k\partial_l \overline{u}_j + \frac{\overline{\Delta}^6}{3!}\, \partial_k\partial_l\partial_m \overline{u}_i\ \partial_k\partial_l\partial_m \overline{u}_j + \dots \ . \tag{4}$$

For 3-D LES, it would be very expensive (both in terms of memory and CPU requirements) to keep many terms in this expansion. In that respect, an already very interesting candidate model for LES is the one corresponding to truncation of the expansion to the first term:

$$\tau_{ij}^M = \overline{\Delta}^2\, \partial_k \overline{u}_i\, \partial_k \overline{u}_j \ . \tag{5}$$

This non-linear isotropic model was not included in the LES models evaluated in *a priori* tests in Clark *et al.* (1979), McMillan & Ferziger (1979), Bardina *et al.* (1983), Lund & Novikov (1992), Salvetti & Banerjee (1995), some of which were revisited in Winckelmans *et al.* (1996). It has, however, already been tested *a priori* against experimental data (unfortunately, 2-D cuts) in Liu *et al.* (1994) with correlation levels of about 0.7, and against DNS data in Borue & Orszag (1998) with correlation levels between 0.83 and 0.97 (*i.e.*, very high!) depending on the type of smooth filter used and on the filter size. It is also argued in Liu *et al.* (1994) that this model has some ties with the Bardina (1983) scale-similarity model, $\tau_{ij}^M = L_{ij} = \overline{\overline{u}_i \overline{u}_j} - \overline{\overline{u}}_i \overline{\overline{u}}_j$. The link also appears in an appendix in Horiuti (1997) where we observe that the first term in the approximate expansion of L_{ij} is indeed the same as the first term in the exact Leonard expansion. The other terms are, however, very different. The Leonard model (truncated to one term or more) is thus not identical to the Bardina model. Nevertheless, we recall that, for smooth filtering such as the Gaussian or the top hat, the Bardina model also exhibits a high level of correlation with the exact stress: *e.g.*, 0.8 in Liu *et al.* (1994), 0.7 in Gaussian filtered DNS in Winckelmans *et al.* (1996), but only 0.5-0.6 in Liu *et al.*

(1994) when "approximating" the Bardina model by using $\tau_{ij}^M \simeq L_{ij} = \widehat{\overline{u}_i \overline{u}_j} - \widehat{\overline{u}}_i \widehat{\overline{u}}_j$ where the second filter width, $\widehat{\Delta}$, is now taken as twice the original filter width, $\overline{\Delta}$. In *a priori* tests with smooth filters, it thus appears that the one-term Leonard model consistently produces higher levels of correlation than the Bardina model.

Finally, it can also be shown (Carati *et al.*, 1998) that, for all filters that are C^∞ in wave space and have non-zero second moment (that is most of the filters defined in physical space, such as the Gaussian, the top hat, all discrete filters, etc.), there exists a generalized Leonard expansion that always starts with

$$\tau_{ij} = \overline{\Delta}^2 \, \partial_k \overline{u}_i \, \partial_k \overline{u}_j + \dots \; . \tag{6}$$

where the filter width is normalized as follows:

$$\overline{\Delta}^2 = \int_\infty^\infty x^2 \, \overline{G}(x) \, dx = -\frac{d^2 \overline{G}}{dk^2}|_{k=0} \; . \tag{7}$$

Hence, the present investigation (theoretical and numerical) using the one-term Leonard model is not limited to the Gaussian filter; this model is truly generic. An important exception (because it is still used so often in spectral LES) is the sharp cutoff "filter" applied in wave space. This "filter" has very poor properties in physical space; it doesn't even have a second order moment. It does not allow for any kind of generalized Leonard expansion, or even any kind of one-term Leonard model, because it totally removes all information beyond the sharp cutoff. We also recall that no significant correlation with DNS data are obtained when testing the Bardina model with the sharp cutoff filter.

It should also be noted that an original integral formulation of the one-term Leonard model has been developed and tested by Cottet (1997a,b), following developments in vortex methods (Cottet, 1996). Its further investigation was the object of parallel study during this Summer Program.

When used in the filtered NS equations, the one-term Leonard model behaves as a non-linear diffusion/antidiffusion model. Indeed, it is easily seen (Leonard, 1997) that

$$-\partial_j \tau_{ij}^M = -\overline{\Delta}^2 \, \overline{S}_{jk} \, \partial_j \partial_k \overline{u}_i \; , \tag{8}$$

so that $\overline{S}_{jk}$ plays the role of a tensorial viscosity for the filtered velocity field. This tensor is not positive-definite. Transforming to the principal coordinates, $\mathbf{x}'$, of $\overline{S}_{jk}$, one obtains (Leonard 1997):

$$-\overline{S}_{jk} \, \partial_j \partial_k \overline{f} = -\left(\alpha_1 \, \partial_{1'} \partial_{1'} + \alpha_2 \, \partial_{2'} \partial_{2'} + \alpha_3 \, \partial_{3'} \partial_{3'}\right) \overline{f} \; . \tag{9}$$

Since the eigenvalues of $\overline{S}_{jk}$, $(\alpha_1, \alpha_2, \alpha_3)$, satisfy $\alpha_1 + \alpha_2 + \alpha_3 = 0$, one has effectively negative diffusion along the stretching direction(s). This corresponds to local directional backscatter.

Let's examine the energy transfer and the dissipation. One easily obtains:

$$\partial_t \left(\frac{\overline{u}_i \overline{u}_i}{2} \right) + \partial_j \left(\left(\overline{P} + \frac{\overline{u}_i \overline{u}_i}{2} \right) \overline{u}_j + \overline{u}_i \left(\tau_{ij} - 2\nu \, \overline{S}_{ij} \right) \right) = -\epsilon \; , \tag{10}$$

with $\epsilon = -\tau_{ij}\overline{S}_{ij} + 2\nu\,\overline{S}_{ij}\overline{S}_{ij}$. The term $\partial_j(\cdots)$ represents the convective contribution to the energy flux, while ϵ represents the local energy flux: (1) the flux from large (and less filtered) scales to small (and more filtered) scales: effective dissipation if positive, effective backscatter if negative; and (2) the dissipation due to the molecular viscosity: clearly always positive. For homogeneous turbulence, the convective contribution has no net effect. We then write, for the global dissipation rate,

$$\frac{d\overline{E}}{dt} = \frac{d}{dt}\langle\frac{\overline{u}_i\overline{u}_i}{2}\rangle = -\langle\epsilon\rangle\ . \tag{11}$$

For uniform ν, the global dissipation due to viscosity is also obtained as

$$\langle\epsilon^\nu\rangle = \nu\,\langle 2\overline{S}_{ij}\overline{S}_{ij}\rangle = 2\nu\,\langle\frac{\overline{\omega}_i\overline{\omega}_i}{2}\rangle = 2\nu\,\overline{\mathcal{E}} \tag{12}$$

where $\overline{\omega}_i = \epsilon_{ijk}\partial_j\overline{u}_k$ (with ϵ_{ijk} the permutation tensor) is the filtered vorticity field and $\overline{\mathcal{E}}$ is the global enstrophy.

The contribution of the Leonard model to the local energy flux (dissipation or backscatter) is (Leonard, 1997; Borue & Orszag, 1998):

$$\begin{aligned}\epsilon^M = -\tau_{ij}^M\,\overline{S}_{ij} &= -\overline{\Delta}^2\,\partial_k\overline{u}_i\,\partial_k\overline{u}_j\overline{S}_{ij}\\ &= -\overline{\Delta}^2\,\left(\overline{S}_{ki}\overline{S}_{ij}\overline{S}_{jk} - \overline{R}_{ki}\overline{S}_{ij}\overline{S}_{jk}\right)\\ &= \overline{\Delta}^2\,\left(\frac{1}{4}\overline{\omega}_i\overline{S}_{ij}\overline{\omega}_j - \mathrm{tr}\left(\overline{S}^3\right)\right)\ .\end{aligned} \tag{13}$$

where $\overline{R}_{ij} = \left(\partial_j\overline{u}_i - \partial_i\overline{u}_j\right)/2 = -\epsilon_{ijk}\overline{\omega}_k/2$ is the antisymmetric rate of rotation tensor. This contribution is not necessarily positive, hence the natural backscatter provided by the model.

For homogeneous turbulence, the global contribution of the model is, however, dissipative as $\langle\epsilon^M\rangle$ is proportional to the negative of the global skewness. A sufficient condition to ensure global dissipation is thus that the global skewness of the LES field remains negative (the necessary condition being that $\langle\epsilon^\nu + \epsilon^M\rangle \geq 0$). The skewness is indeed negative in homogeneous turbulence and its DNS. It should also be negative in good LES. It was indeed found to remain negative in all LES's of decaying homogeneous turbulence that we conducted during the present investigation, these LES's being started from a filtered DNS field and thus having a negative global skewness initially. If one starts a DNS or a LES from a random field with Gaussian statistics, then the skewness is initially zero. However, as the simulation proceeds, it quickly becomes negative because the flow develops into "real" turbulence.

The one-term Leonard model could be constrained locally by putting a limiter on the directional negative diffusion: find the eigenvalues and eigenvectors of the local strain rate tensor, express the forcing term, $-C\,\overline{\Delta}^2\,\overline{S}_{jk}\partial_j\partial_k\overline{u}_i$ in this system of coordinates, and ignore (*i.e.*, clip) the direction(s) corresponding to negative diffusion. This certainly makes the model anisotropic. Notice that there is now a need for a new unknown parameter C. Indeed, since this "clipping" corresponds to a

major alteration of the original Leonard model, there is no reason to expect, *a priori*, that $C = 1$. Of course, this clipping approach can be refined further by enforcing that the total forcing term $\left(\nu\partial_j\partial_j - C\,\overline{\Delta}^2\,\overline{S}_{jk}\partial_j\partial_k\right)\overline{u}_i$ be clipped in the direction(s) corresponding to net negative diffusion. We notice, in passing, that the integral formulation developed by Cottet (1996, 1997a,b) essentially allows for convenient directional clipping without having to compute eigenvalues and eigenvectors.

Alternatively, one could clip the Leonard model isotropically by enforcing that $\epsilon^M \geq 0$ at each point. Defining $m_{ij} = \overline{\Delta}^2\,\partial_k\overline{u}_i\partial_k\overline{u}_j$, the model could be written as

$$\begin{aligned} \tau_{ij}^M &= C\,m_{ij} \qquad \text{if} \qquad -m_{ij}\overline{S}_{ij} \geq 0\,, \\ \tau_{ij}^M &= C\left[m_{ij} - \frac{\left(m_{kl}\overline{S}_{kl}\right)}{\left(\overline{S}_{kl}\overline{S}_{kl}\right)}\,\overline{S}_{ij}\right] \qquad \text{otherwise}\,. \end{aligned} \tag{14}$$

Again, there is a parameter C, and one can also refine this approach. For both clipping approaches, the determination of the parameter could be done using a dynamic procedure.

In any case, "clipping" guarantees pure dissipation (and hence numerical stability), but it isn't justified theoretically. Here, we wish to first investigate the unaltered model: no clipping. With good numerics, and assuming that the computation doesn't blow up, the hope is that such a model could indeed provide for reasonable local backscatter while remaining globally sufficiently dissipative. One could argue that, in principle, the unclipped one-term Leonard model is numerically ill-conditioned. Our numerical experience so far (decaying homogeneous turbulence and channel flow) is that the simulations do not blow up, confirming our hope that LES's with that model and without limiter (*i.e.*, with local backscatter) can indeed be carried out successfully. This is very good news. This result is probably due, in part, to the fact that the direction(s) of negative diffusion evolve in space and time while the simulation proceeds. The negative diffusion (which is certainly numerically unstable if applied forever) here constantly changes direction and is counterbalanced by positive diffusion. In a way, the simulation corresponds to dynamic dissipation events happening together with dynamic backscatter events, the mean remaining globally dissipative.

However, in our pseudo-spectral LES of decaying isotropic turbulence at high Re_λ, the one-term Leonard model, when used on its own, is found to provide too little global dissipation, see Figs. 3 to 5 (even though the simulation doesn't blow up). This is seen even more clearly when comparing the evolution of the LES energy spectrum with the DNS, see Figs. 7 to 9. Thus, we find that the one-term Leonard model does not suffice in actual LES runs. Hence, it was decided to develop and test a mixed model: add to the one-term Leonard model a purely dissipative term such as the dynamic Smagorinsky term:

$$\tau_{ij}^M = \overline{\Delta}^2\,\partial_k\overline{u}_i\,\partial_k\overline{u}_j - 2\,C\,\overline{\Delta}^2\,\left(2\overline{S}_{kl}\overline{S}_{kl}\right)^{1/2}\,\overline{S}_{ij}\,. \tag{15}$$

This is done in the same spirit as Zang *et al.* (1993) for the mixed model contructed by adding a dynamic Smagorinsky term to the Bardina model. See also

Horiuti (1997) for yet another two-parameter dynamic mixed model. This mixed model proposed here is still isotropic as opposed to non-isotropic models such as Carati & Cabot (1996) or Cottet (1997a,b). The first term is expected to be "the good filtered-scales model" because (1) it has some solid mathematical basis (see above) and (2) it naturally provides for local backscatter (as LES models should, see also Carati *et al.*, 1995a). On its own, however, it does not provide for enough dissipation. Conversely, the second term (with the classical Smagorinsky, 1963, $1/T$ scaling, $\left(2\overline{S}_{kl}\overline{S}_{kl}\right)^{1/2}$, such as above; or with the Kolmogorov scaling proposed by Carati *et al.*, 1995b, and tested in actual LES, *e.g.*, Dantinne *et al.*, 1998; or with other scalings,*e.g.*, see a review in Winckelmans *et al.*, 1996) has long been known to be a poor model that always produces local dissipation (when C is constrained to remain positive). For the proposed mixed model, we now have:

$$\epsilon^M = -\tau_{ij}^M \overline{S}_{ij} = -\overline{\Delta}^2\, \partial_k \overline{u}_i\, \partial_k \overline{u}_j\, \overline{S}_{ij} + C\, \overline{\Delta}^2\, \left(2\overline{S}_{ij}\overline{S}_{ij}\right)^{3/2} \quad . \tag{16}$$

When the Smagorinsky term is used on its own as a LES model together with the dynamic procedure (Germano *et al.*, 1991; Ghosal *et al.*, 1992, 1995; Moin *et al.*, 1994), it doesn't necessarily lead to the correct dissipation as compared to the DNS; it very much depends on the filter used, see the results below, Figs. 3 to 5. We here wish to stress that, in the present approach, we really consider the one-term Leonard model as "the filtered-scales model" and the dynamic Smagorinsky term as an added numerical aid for enhancing the local dissipation. Although there is some similarity between the second possible clipped model presented above and the present mixed model, there are significant differences. The formulation of the mixed model is continuous (no "if" statement). Moreover, in the mixed model, the added term with dynamic C is not a clipping of the first term as C does not multiply both terms. As a consequence, the new mixed model is still isotropic, and it still allows for local backscatter; ϵ^M is not necessarily positive. Of course, the amount of local backscatter allowed is now less than for the pure Leonard model, and the dissipation is now more. Notice that the first term (the "model") still has the known coefficient coming from the Leonard expansion with the chosen smooth LES filter (e.g., Gaussian). In all we do here, it is with that same chosen LES filter that we filter the DNS results in order to compare them with the LES results (or, conversely, that we de-filter the LES results to compare them with the DNS results).

Whether the dynamically obtained C in this new mixed model will lead to the proper amount of dissipation as compared to DN, remains to be seen (see the results section). In that respect, for identical LES filters, it had better be that the dynamic C obtained in the mixed model turns out to be smaller than the dynamic C obtained when using the Smagorinsky term on its own as LES model. As mentioned above, C is here obtained through the dynamic procedure (Germano *et al.*, 1991; Ghosal *et al.*, 1992, 1995; Moin *et al.*, 1994) by (1) applying an additional test filter, $\widehat{G}$, which is such that the combined "LES + test" filter, $\widehat{\overline{G}}$, is similar the original LES filter, $\overline{G}$; (2) assuming similarity of the LES models at both levels, τ_{ij}^M similar to T_{ij}^M, with the same C; and (3) satisfying Germano's identity, $T_{ij} - \widehat{\tau}_{ij} = L_{ij} = \widehat{\overline{u}_i \overline{u}_j} - \widehat{\overline{u}}_i \widehat{\overline{u}}_j$, in

the least-square sense: $\langle E_{ij}E_{ij}\rangle$, where $E_{ij} = \left(T_{ij}^M - \widehat{\tau}_{ij}^M\right) - L_{ij}$, is minimized, with integration $\langle\ldots\rangle$ done over the homogeneous direction(s). C is thus uniform along the homogeneous direction(s). Moreover, along the non-homogeneous direction(s) (if any), it is also assumed that the spatial variation of C with respect to the test filter can be factored out, *i.e.*, that $\widehat{C\,a_{ij}} \simeq C\,\widehat{a}_{ij}$. This requirement is trivially satisfied if the test filter is only applied along the homogeneous direction(s), as is often the case in practice (but then the assumed similarity between the LES and LES+test filters is not strictly correct). Otherwise, it is only a (poor) assumption that should be validated *a posteriori* (at least statistically, when averaged over time).

Here, working in wave space, we take $\widehat{\overline{G}}(k) = \exp\left(-\alpha^2\,k^2\overline{\Delta}^2/2\right)$, *i.e.*, $\widehat{\overline{\Delta}}/\overline{\Delta} = \alpha > 1$, which is indeed similar to $\overline{G}(k) = \exp\left(-k^2\overline{\Delta}^2/2\right)$. The required test filter is also Gaussian: $\widehat{G}(k) = \widehat{\overline{G}}(k)/\overline{G}(k) = \exp\left(-\left(\alpha^2-1\right)\,k^2\overline{\Delta}^2/2\right)$, *i.e.*, $\widehat{\overline{\Delta}}/\overline{\Delta} = \sqrt{\alpha^2-1}$. Typically, we use $\alpha = 2$. Another filter is the top hat filter: $\overline{G}(k) = \sin\left(\sqrt{3}\,k\overline{\Delta}\right)/\left(\sqrt{3}\,k\overline{\Delta}\right)$, and thus $\widehat{\overline{G}}(k) = \sin\left(\sqrt{3}\,k\widehat{\overline{\Delta}}\right)/\left(\sqrt{3}\,k\widehat{\overline{\Delta}}\right)$. If we choose $\alpha = 2$, the test filter becomes $\widehat{G}(k) = \widehat{\overline{G}}(k)/\overline{G}(k) = \cos\left(\sqrt{3}\,k\widehat{\overline{\Delta}}\right)$ (Carati, 1997). This test filter is also easily applied in physical space using only grid values as it is the discrete "arithmetic mean": $\widehat{G}(x) = \left(\delta\left(x+\sqrt{3}\,\overline{\Delta}\right) + \delta\left(x-\sqrt{3}\,\overline{\Delta}\right)\right)/2$. Of course, one needs to choose $\overline{\Delta}$ so that $\sqrt{3}\,\overline{\Delta}$ is a multiple of the grid size Δ.

The dynamic procedure for the mixed model is summarized here as:

$$
\begin{gathered}
m_{ij} = \overline{\Delta}^2\,\partial_k\overline{u}_i\,\partial_k\overline{u}_j\ , \quad a_{ij} = 2\,\overline{\Delta}^2\,\left(2\overline{S}_{kl}\overline{S}_{kl}\right)^{1/2}\,\overline{S}_{ij}\ , \quad \tau_{ij}^M = m_{ij} - C\,a_{ij}\ , \\
M_{ij} = \widehat{\overline{\Delta}}^2\,\partial_k\widehat{\overline{u}}_i\,\partial_k\widehat{\overline{u}}_j\ , \quad A_{ij} = 2\,\widehat{\overline{\Delta}}^2\,\left(2\widehat{\overline{S}}_{kl}\widehat{\overline{S}}_{kl}\right)^{1/2}\,\widehat{\overline{S}}_{ij}\ , \quad T_{ij}^M = M_{ij} - C\,A_{ij}\ , \\
p_{ij} = L_{ij} + \left(\widehat{m}_{ij} - M_{ij}\right)\ , \quad q_{ij} = \left(\widehat{a}_{ij} - A_{ij}\right)\ , \quad C = \frac{\langle p_{ij}\,q_{ij}\rangle}{\langle q_{ij}\,q_{ij}\rangle}\ .
\end{gathered}
\tag{17}
$$

For homogeneous turbulence, all three directions are homogeneous so that $C = C(t)$. For the channel flow, two directions are homogeneous so that $C = C(y,t)$. Since the channel flow dynamical LES eventually reaches statistical equilibrium, time averaging can also be done at some point, and one ends up with a profile, $C = C(y)$. Then the dynamic procedure assumption above is statistically better verified.

Notice that the added dissipative term in the mixed model is formally of the same order as the one-term Leonard model: both involve product of first derivatives of the LES field. Since dynamic hyper-viscosity models such as

$$
\tau_{ij}^M = 2\,C\,\overline{\Delta}^4\,\left(2\overline{S}_{kl}\overline{S}_{kl}\right)^{1/2}\,\partial_m\partial_m\overline{S}_{ij}
\tag{18}
$$

have also been used with some success in LES (*e.g.*, Winckelmans *et al.*, 1996, in *a priori* tests; Dantinne *et al.*, 1998, in actual LES with sharp cutoff test filtering), we also investigated the following possibility of mixed model:

$$
\tau_{ij}^M = \overline{\Delta}^2\,\partial_k\overline{u}_i\,\partial_k\overline{u}_j + 2\,C\,\overline{\Delta}^4\,\left(2\overline{S}_{kl}\overline{S}_{kl}\right)^{1/2}\,\partial_m\partial_m\overline{S}_{ij}\ ,
\tag{19}
$$

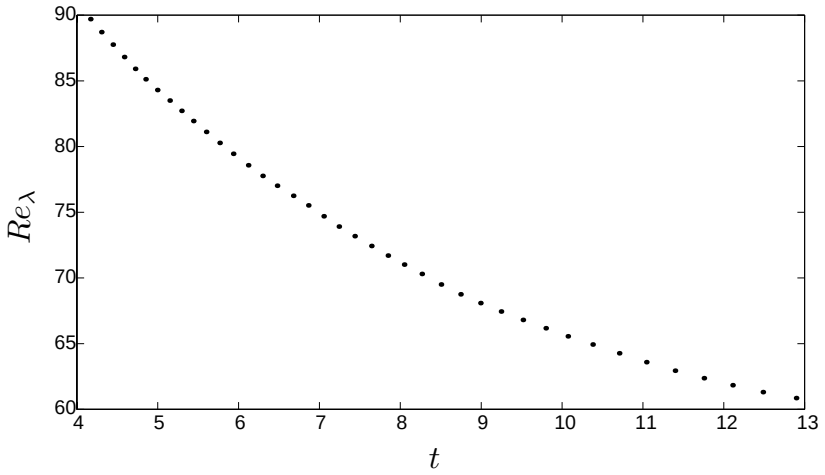

FIGURE 1. $Re_\lambda(t)$ for the reference 256^3 DNS.

where the added term now clearly involves higher order derivatives and is thus expected to only affect the high-end of the energy spectrum. When tested numerically with Gaussian filtering, this mixed model did not dissipate enough energy.

2. Results for decaying homogeneous turbulence

For the LES tests on decaying homogeneous turbulence, the solver is a dealiased pseudo-spectral code. The reference data is a 256^3 DNS at high Re_λ that was run using the same spectral code. The DNS was started using a field with given spectra and random phases. This initial condition then evolved into real turbulence. The usable reference DNS data then covers the window of Re_λ shown in Fig. 1. At the begining ($t = 4.17$, $Re_\lambda \approx 90$), the Kolmogorov scale, $\eta = \left(\nu^3/\langle\epsilon\rangle\right)^{1/4}$, is such that $k_{\max}\,\eta \approx 2$; the DNS is thus well-resolved. At the end ($t = 13.32$), $k_{\max}\,\eta \approx 4$. The $t = 4.17$ DNS was Gaussian filtered using $\overline{\Delta} = 2\sqrt{2}\,\Delta_{256}$, and was then further truncated to 64^3 (*i.e.*, $\overline{\Delta} = \Delta_{64}/\sqrt{2}$) to be used as an initial condition for the LES runs. Hence, at the maximum wavenumber of the truncated set, we have $\overline{G} = \exp\left(-\pi^2/4\right) = 0.085$; the 64^3 grid used to resolve the LES thus covers well the range where the LES filter is significant while not overkilling it. At half the maximum wavenumber, we have $\overline{G} = 0.54$. For the dynamic procedure, we used the classical value $\alpha = 2$. We also tried $\alpha = \sqrt{2}$, but the results were consistently slightly better with $\alpha = 2$.

As a first test of the one-term Leonard model, the correlation between the model, $\tau_{ij}^M = \overline{\Delta}^2 \partial_k \overline{u}_i \partial_k \overline{u}_j$, and the exact stress, τ_{ij}, was evaluated using the filtered DNS data. It came out very high, 0.92, in good agreement with correlations in Borue & Orszag (1998). That is certainly a victory for the one-term Leonard model, at least in such *a priori* testing. It shows that the expansion truncated to one term already contains most of the stress.

Notice that the correlation measures the alignement between the two stresses. It doesn't say anything about the "best" coefficient to use in front of the model. Since the original Leonard expansion has been truncated to one term, it is valid

to ask if this term shouldn't be rescaled somehow. Hence, as a second test of the one-term Leonard model, the dynamic procedure was applied to an assumed $\tau_{ij}^M = C\,\overline{\Delta}^2 \partial_k \overline{u}_i \partial_k \overline{u}_j$. The result came out to be $C = 1.0050$, pretty close to $C = 1$ indeed (difference of 0.5%). This is a double victory: one for the theoretical developments that claim that the good value is $C = 1$, and one for the dynamic procedure that indeed finds that value.

Filtering the DNS even more was also considered. With $\overline{\Delta}$ twice as large as above, the correlation came out as 0.89 and the dynamic C came out as $C = 0.9536$ (difference of 5%: not as good, but still very close. This filter size is probably too large with respect to the Kolmogorov scale of this high Re_λ turbulence.

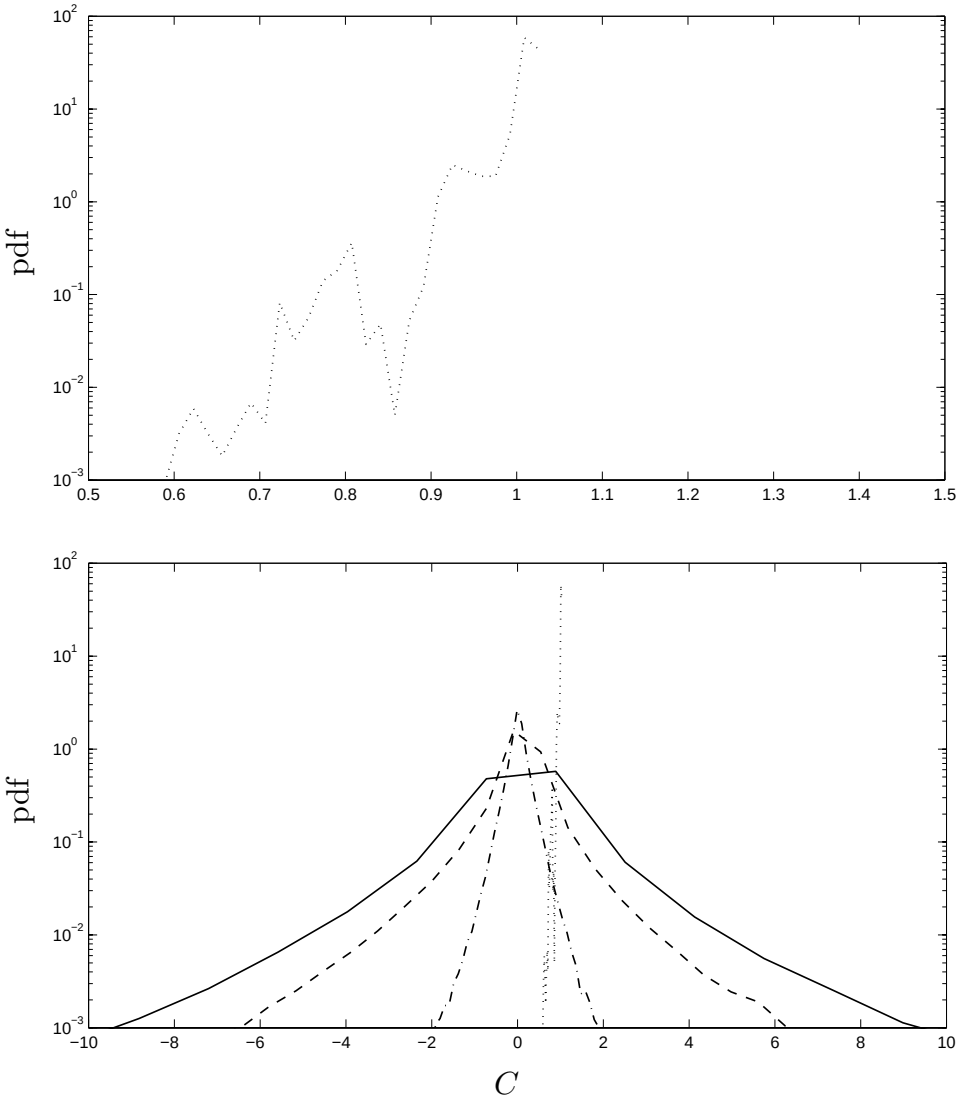

FIGURE 2. Pdf of the model coefficient, C: dynamic Leonard model, Gaussian: ····· ; Leonard model + dynamic Smagorinsky term, Gaussian: ——— ; dynamic Smagorinsky model, Gaussian: - - - - ; dynamic Smagorinsky model, sharp cutoff: —·— .

Finally, as a third test of the one-term Leonard model, the dynamic procedure was applied but this time locally (*i.e.*, no averaging over the homogeneous directions). The obtained pdf of C is given in Fig. 2. The striking result is that the pdf is extremely sharp, with prefered value: $C \approx 1$. Notice that the pdf is not symmetric; it is skewed to the left. Notice also that there are no negative C. Again, this is a victory of the model and of the local dynamic procedure. For comparison, we also provide the pdf of the Smagorinsky term when used as the LES model. Two cases are examined: Gaussian filtering and sharp cutoff filtering. In both cases, the obtained pdf is very wide with many negative C values, confirming that the Smagorinsky term is indeed a poor LES model.

From this *a priori* study, it certainly appears that there is no point in having something other than $C = 1$ in front of the one-term Leonard model. This is why the mixed model presented above only has one parameter: the one in front of the added dynamic Smagorinsky term. Notice that Fig. 2 also provides the pdf of that C; as expected, it is very wide, even wider than when the Smagorinsky term is used as LES model. This is to be expected since the Leonard term in the hybrid model is "the LES model", the remainder dynamic Smagorinsky term being added for enhancing dissipation with little pretention on actual LES modeling.

The results obtained when using the mixed model (Leonard model + dynamic Smagorinsky term) with Gaussian filtering are presented in Figs. 3 to 10. They are compared with (1) the DNS, (2) the Leonard model with Gaussian filtering, (3) the dynamic Smagorinsky model with Gaussian filtering, and (4) the dynamic Smagorinsky model with sharp cutoff filtering (often used in spectral LES). For fair comparison (quality versus computational cost), all LES's are run using the same resolution: 64^3. Moreover, for the LES's with Gaussian filtering, the quantities such as resolved energy spectra, $E(k)$, resolved energy, $E = \int_0^{k_{\max}} E(k)\, dk$, and resolved enstrophy, $\mathcal{E} = \int_0^{k_{\max}} k^2\, E(k)\, dk$, are evaluated by "defiltering" the LES results, i.e., by using $E(k) = \overline{E}(k)\, \exp\left(k^2 \overline{\Delta}^2\right)$. This allows for straighforward comparison with the DNS and the sharp cutoff Smagorinsky LES. (Of course, another way would be to Gaussian filter the DNS and the sharp cutoff LES.)

The Leonard model with Gaussian filtering, when used on its own, does not blow up. However, it provides too little dissipation, see Figs. 3 and 5, even at the start. Thus, although the initial correlation between τ_{ij}^M and τ_{ij} is very high (0.92), the global model dissipation, $-\langle \tau_{ij}^M \overline{S}_{ij} \rangle$, is substantially lower than the exact filtered-scales dissipation, $-\langle \tau_{ij} \overline{S}_{ij} \rangle$ (here, at the start, 4.112 versus 6.773). As expected, the global model dissipation is positive since the global skewness of the LES fields is initially negative and remains so. The dynamic sharp cutoff Smagorinsky model leads to too much energy dissipation from the start, see Figs. 3 and 6. The dynamic Smagorinsky model with Gaussian filtering starts off with the correct slope, but it then quickly underdissipates, see Figs. 3 and 5. The mixed model starts off with the correct slope and follows well the energy decay curve, see Figs. 3 and 5. Initially, the total dissipation of the LES, model + viscous, is $(4.112 + 2.887) + 1.5944 = 8.593$, to be compared to 8.367 for the 256^3 filtered DNS: only a 2.7% difference. Notice also

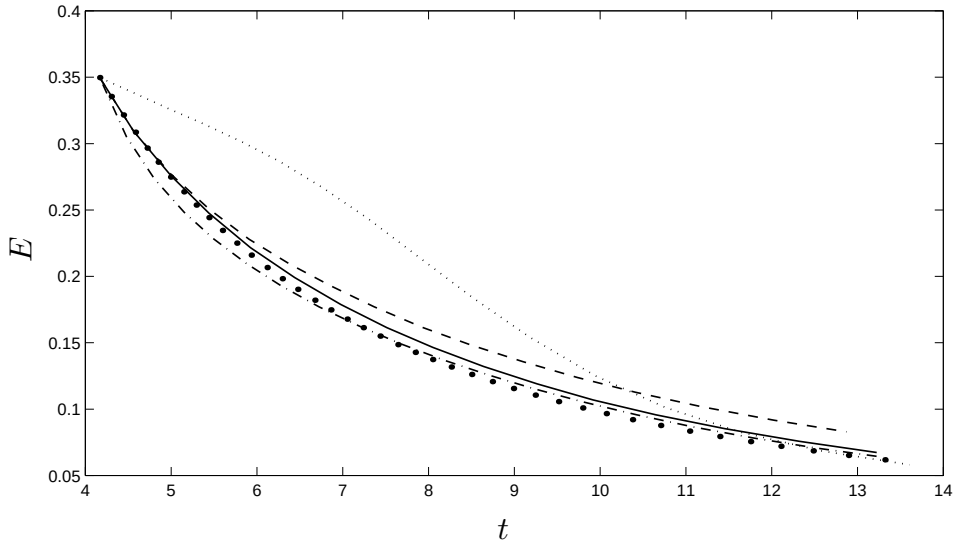

FIGURE 3. Resolved energy, $E(t)$: truncated DNS: • ; Leonard model, Gaussian: ····· ; Leonard model + dynamic Smagorinsky term, Gaussian: ——— ; dynamic Smagorinsky model, Gaussian: – – – – ; dynamic Smagorinsky model, sharp cutoff: —·— .

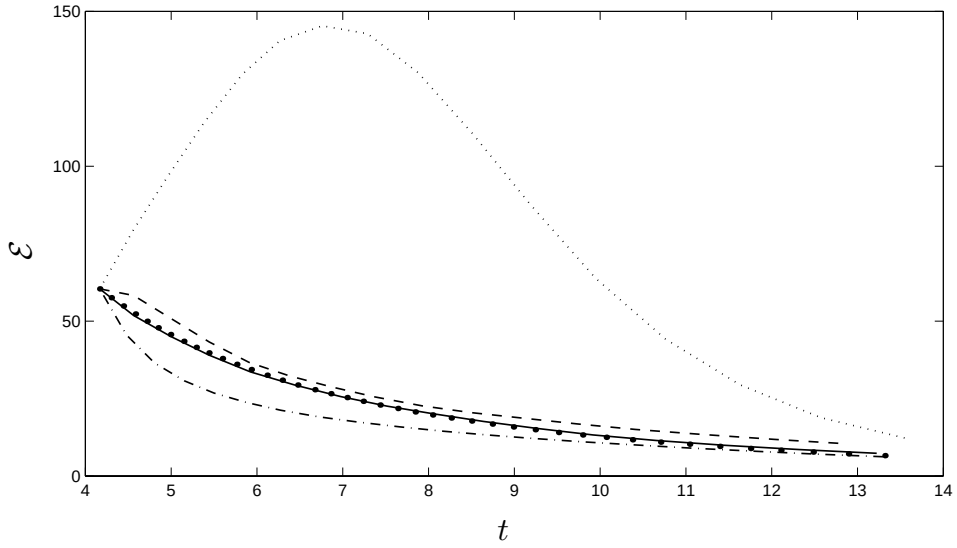

FIGURE 4. Resolved enstrophy, $\mathcal{E}(t)$: truncated DNS: • ; Leonard model, Gaussian: ····· ; Leonard model + dynamic Smagorinsky term, Gaussian: ——— ; dynamic Smagorinsky model, Gaussian: – – – – ; dynamic Smagorinsky model, sharp cutoff: —·— .

the significant contribution of the Leonard term to the model global dissipation; it is larger than the contribution of the dynamic Smagorinsky term: 4.112 versus 2.887. As expected, it is positive since the global skewness of the LES fields is initially negative and remains so.

The differences between the investigated models are even more dramatic when

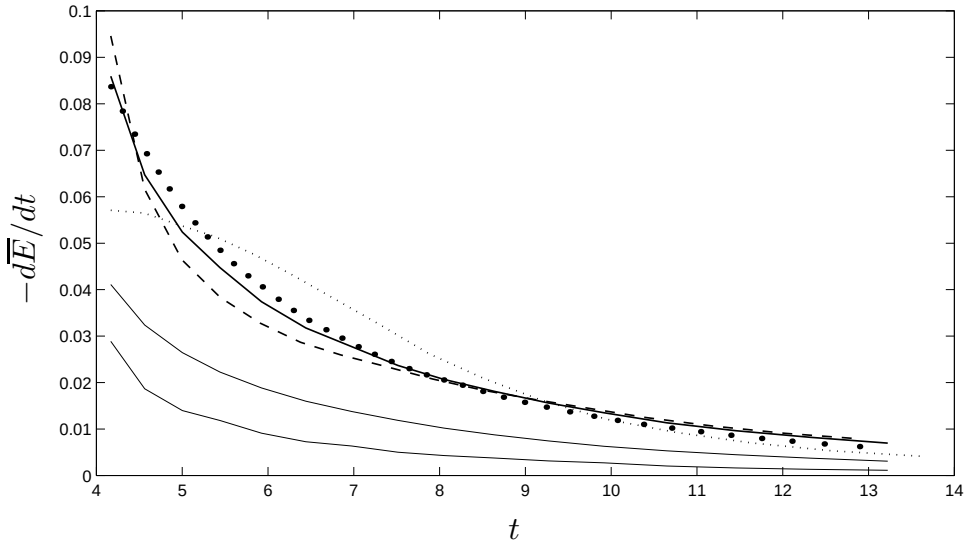

FIGURE 5. Dissipation of resolved energy, $-d\overline{E}/dt = -\langle \tau_{ij}^M \overline{S}_{ij} \rangle + 2\nu \langle \overline{S}_{ij} \overline{S}_{ij} \rangle$: truncated DNS, Gaussian: • ; Leonard model, Gaussian: ····· ; Leonard model + dynamic Smagorinsky term, Gaussian: ——— (Leonard: ——— (thin), Smagorinsky: ——— (thinner)); dynamic Smagorinsky model, Gaussian: - - - - .

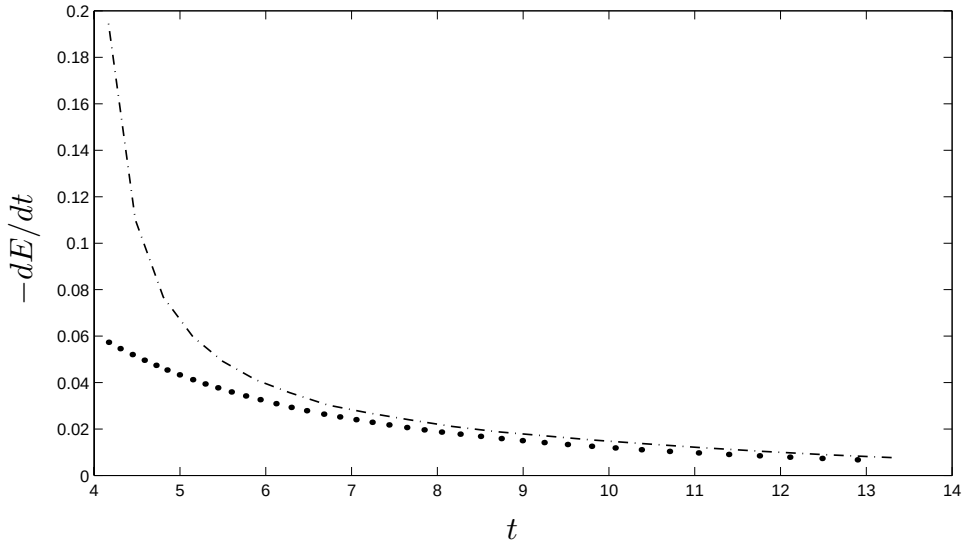

FIGURE 6. Dissipation of resolved energy, $-dE/dt$: truncated DNS, sharp cutoff: • ; dynamic Smagorinsky model, sharp cutoff: —·— .

considering the decay of the enstrophy (which puts more weight on the high-end of the spectrum), see Fig. 4: the dynamic sharp cutoff Smagorinsky model badly misses the initial slope of enstrophy decay (too much decay). Its Gaussian version also misses the initial slope, but on the other side (not enough decay). The mixed model performs very well not only initially, but for the whole course of the simulation; the LES decay curve is almost identical to the DNS curve.

The energy spectra produced by the mixed model are also clearly superior, see

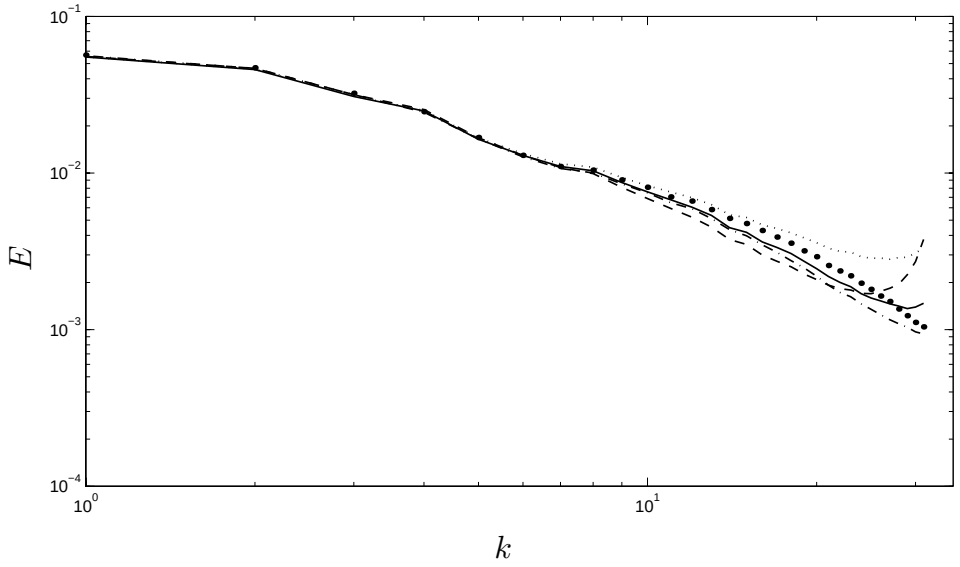

FIGURE 7. Resolved spectrum, $E(k)$, at $t \approx 4.5$: truncated DNS: • ; Leonard model, Gaussian: ····· ; Leonard model + dynamic Smagorinsky term, Gaussian: ——— ; dynamic Smagorinsky model, Gaussian: – – – – ; dynamic Smagorinsky model, sharp cutoff: —·— .

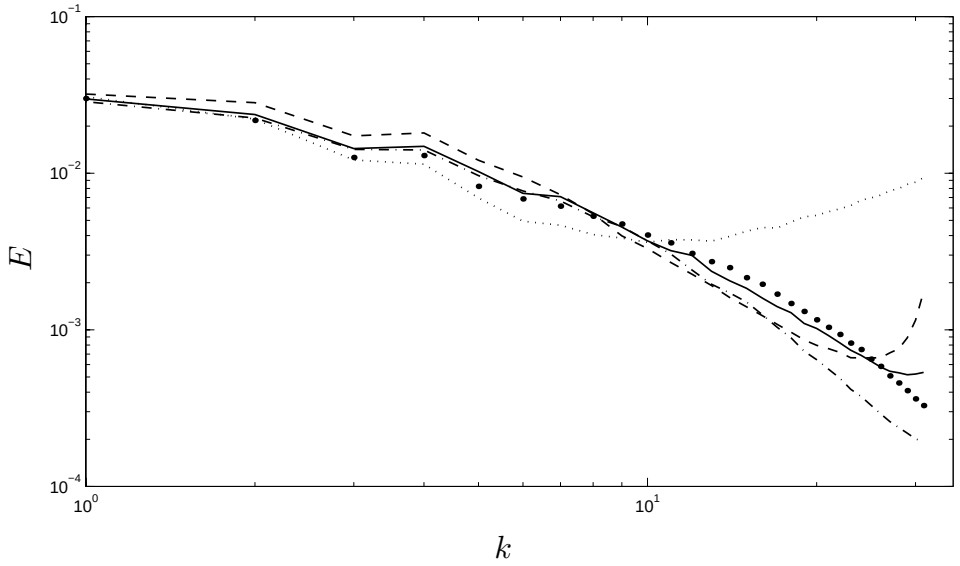

FIGURE 8. Resolved spectrum, $E(k)$, at $t \approx 7.5$: truncated DNS: • ; Leonard model, Gaussian: ····· ; Leonard model + dynamic Smagorinsky term, Gaussian: ——— ; dynamic Smagorinsky model, Gaussian: – – – – ; dynamic Smagorinsky model, sharp cutoff: —·— .

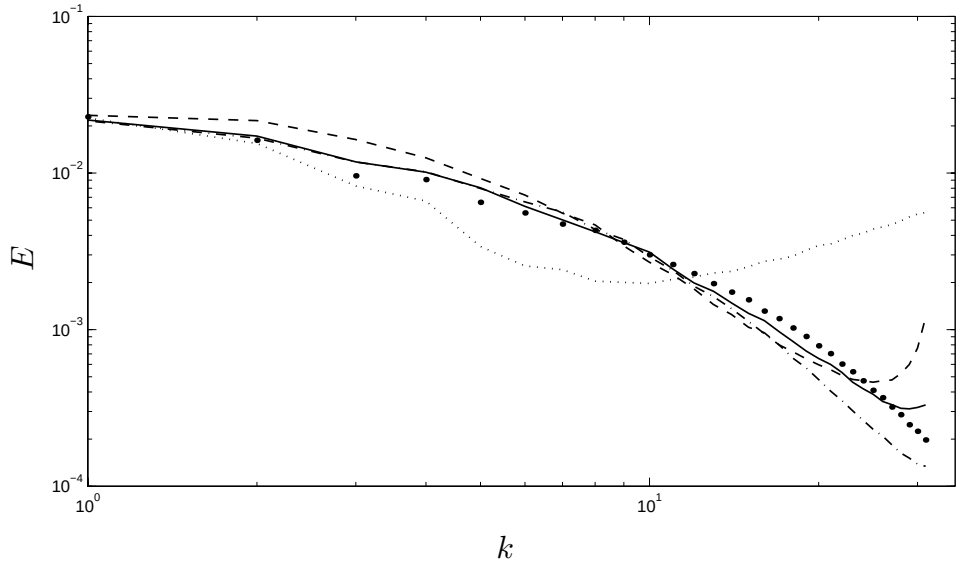

FIGURE 9. Resolved spectrum, $E(k)$, at $t \approx 9.0$: truncated DNS: • ; Leonard model, Gaussian: ····· ; Leonard model + dynamic Smagorinsky term, Gaussian: ——— ; dynamic Smagorinsky model, Gaussian: – – – – ; dynamic Smagorinsky model, sharp cutoff: —·— .

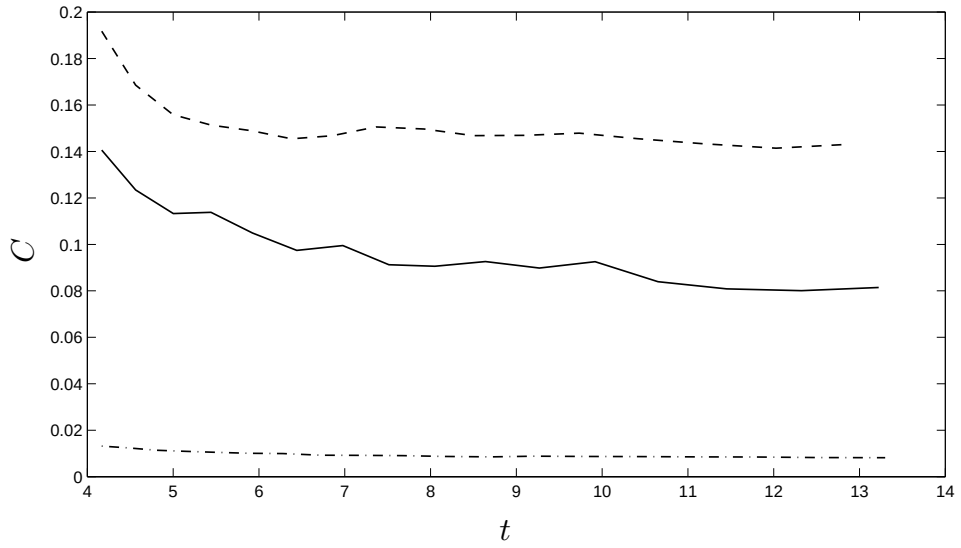

FIGURE 10. Model coefficient, $C(t)$: Leonard model + dynamic Smagorinsky term, Gaussian: ——— ; dynamic Smagorinsky model, Gaussian: – – – – ; dynamic Smagorinsky model, sharp cutoff: —·— .

Figs. 7 to 9; they closely match the DNS spectra over most of the range and for the whole course of the simulation except for the few last wavenumbers (that are here artificially enhanced on the graph because of the "defiltering" mentioned above). The sharp cutoff Smagorinsky model shows some discrepancy in the spectrum, starting at fairly low wavenumbers. Its Gaussian version doesn't perform significantly

better. As to the dynamic model coefficient, Fig. 10, it is seen that the C of the Smagorinsky term in the mixed model is indeed smaller than the C of the Smagorinsky model; the one-term Leonard model thus contributes significantly to the success of the mixed model.

3. Results for the channel flow

For the channel flow investigation, the solver is a fourth order finite difference code. The reference DNS is the AGARD database at $Re_\tau = h\,u_\tau/\nu = 395$ of Mansour *et al.* (1996) (see also Rodi & Mansour, 1993), where h is half the channel width and $u_\tau = \sqrt{\tau_w}$ is the friction velocity with τ_w the mean wall friction. The computational domain is $(L_x, L_y, L_z) = (2\pi, 2, 2\pi/3)h$. The LES filter is chosen as Gaussian in the homogeneous directions, x and z, and top hat in the non-homogeneous direction, y:

$$\overline{G} = \exp\left(-k_x^2\overline{\Delta}_x^2/2\right)\ \frac{\sin\left(\sqrt{3}\,k_y\overline{\Delta}_y\right)}{\left(\sqrt{3}\,k_y\overline{\Delta}_y\right)}\ \exp\left(-k_z^2\overline{\Delta}_z^2/2\right)\ . \tag{20}$$

Hence, the mixed model here becomes

$$\tau_{ij}^M = \overline{\Delta}_x^2\,\partial_x\overline{u}_i\,\partial_x\overline{u}_j + \overline{\Delta}_y^2\,\partial_y\overline{u}_i\,\partial_y\overline{u}_j + \overline{\Delta}_z^2\,\partial_z\overline{u}_i\,\partial_z\overline{u}_j - 2\,C\,\overline{\Delta}^2\ \left(2\overline{S}_{kl}\overline{S}_{kl}\right)^{1/2}\ \overline{S}_{ij}\ , \tag{21}$$

where the "effective" $\overline{\Delta}$ for the added dynamic Smagorinsky term is simply taken as $\left(\overline{\Delta}_x\,\overline{\Delta}_y\,\overline{\Delta}_z\right)^{1/3}$. Notice here another nice feature of the Leonard model: as opposed to the Smagorinsky model, there is no need to define an effective $\overline{\Delta}$. The dynamic procedure is done with $\alpha = 2$. Hence, the test filter here becomes:

$$\widehat{G} = \exp\left(-3\,k_x^2\overline{\Delta}_x^2/2\right)\ \cos\left(\sqrt{3}\,k_y\overline{\Delta}_y\right)\ \exp\left(-3\,k_z^2\overline{\Delta}_z^2/2\right)\ . \tag{22}$$

The test filter is applied in wave space in x and z and in physical space in y (using the arithmetic mean of the two neighbor grid points as explained previously).

For the preliminary runs done so far, the ratios of LES numerical grid to LES filter size are $\Delta_x/\overline{\Delta}_x = 2$, $\Delta_y/\overline{\Delta}_y = \sqrt{3}$ and $\Delta_z/\overline{\Delta}_z = 2$. The LES grid is 48x49x48.

Results on normalized mean profiles as a function of normalized distance to the wall are provided in Figs. 11 to 13: velocity, model stress and model dissipation. With the same smooth filtering, the mixed model outperforms the dynamic Smagorinky model: better mean velocity profile. Notice that the contribution of the Leonard part to the mixed model is significant; for the mean stress, it is higher than the contribution of the dynamic Smagorinsky term; for the mean dissipation, its contribution is higher close to the wall and slightly lower in the core flow. Notice also that the Leonard term contribution to the mean dissipation is indeed positive for all y although it is not necessarily positive locally because of the model backscatter. It is also found that the Leonard fraction of the model stress is essentially linear from the beginning of the log region to the channel center. This behavior is similar to what was obtained by Domaradzki & Saiki (1997) and Domaradzki & Loh (1998)

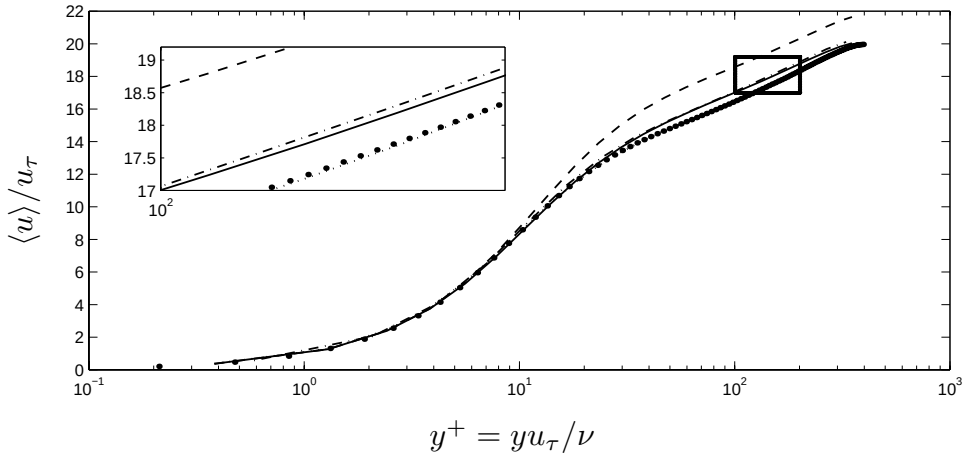

FIGURE 11. Mean velocity profile: DNS: • ; Leonard model + dynamic Smagorinsky term, 48x49x48, Gaussian and top hat: ——— ; dynamic Smagorinsky model, 48x49x48, Gaussian and top hat: - - - - ; dynamic Smagorinsky model, 32x33x32, sharp cutoff: —·— ; dynamic Smagorinsky model, 48x49x48, sharp cutoff: ····· .

using their LES subgrid-scale estimation model and comparing with filtered DNS data. This behavior is different from the behavior of the dynamic Smagorinky term (when used in the mixed model) or model (when used on its own), see Fig. 12.

However, when running a 48x49x48 LES using the Smagorinsky model with sharp cutoff test filtering in x and z and no test-filtering in y, the obtained mean velocity profile is closer to the DNS than for the mixed model with the smooth filtering and filter size used so far. That doesn't necessarily mean that the Smagorinsky model with sharp cutoff is superior. But it certainly calls for further study of the mixed model by investigating other ratios of numerical grid to filter size, other filters, and the effect of the y-grid non-uniformity (see, *e.g.*, Ghosal & Moin, 1995). It also calls for further *a priori* testing of the Leonard and mixed models using DNS of channel flows. This work is still in progress.

We provide in Fig. 14 the mean stress profile for the LES done using the mixed model. The different terms add up to the linear profile for the total stress as expected. Close to the wall, the main contribution is the one due to the viscous stress. Away from the wall, the main contribution is the "Reynolds" stress: $\langle \overline{u} \rangle \langle \overline{v} \rangle - \langle \overline{u}\,\overline{v} \rangle$. For the remainder (total stress minus Reynolds stress), the model contribution away from the wall is significantly higher than the viscous contribution, the Leonard contribution being itself higher than the Smagorinsky contribution. For comparison, Fig. 15 provides the mean stress profile when using the Smagorinsky model with same smooth filtering. Again, the model contribution is higher than the viscous contribution in the core flow.

Figures 16 and 17 provide the mean dissipation profiles: model contribution and viscous contribution. The viscous contribution is dominant close to the wall but is dominated by the model in the core flow. There are significant differences between the mixed model and the Smagorinky model as far as profiles of model versus viscous dissipation are concerned.

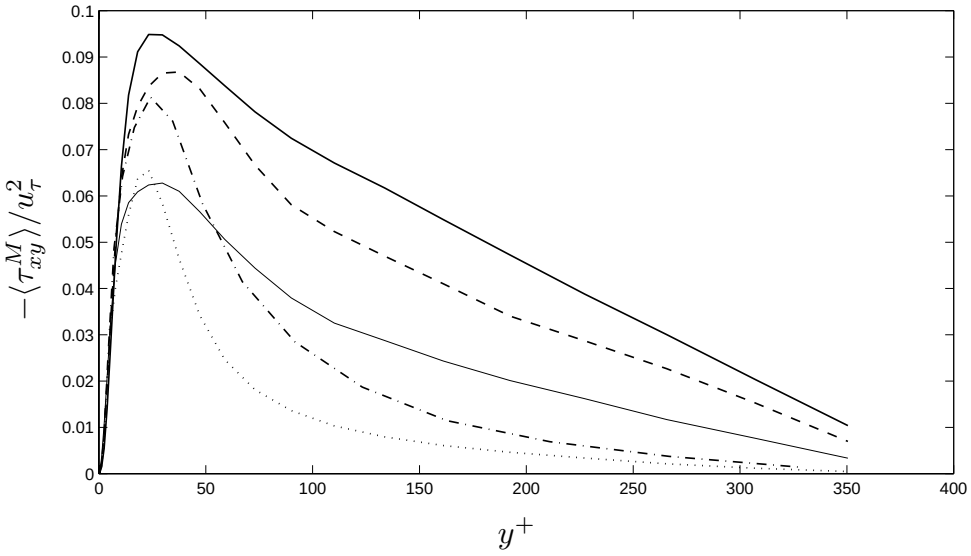

FIGURE 12. Mean model stress profile: Leonard model + dynamic Smagorinsky term, 48x49x48, Gaussian and top hat (Leonard: ——— , Smagorinsky: ———); dynamic Smagorinsky model, 48x49x48, Gaussian and top hat: – – – – ; dynamic Smagorinsky model, 32x33x32, sharp cutoff: —·— ; dynamic Smagorinsky model, 48x49x48, sharp cutoff: ····· .

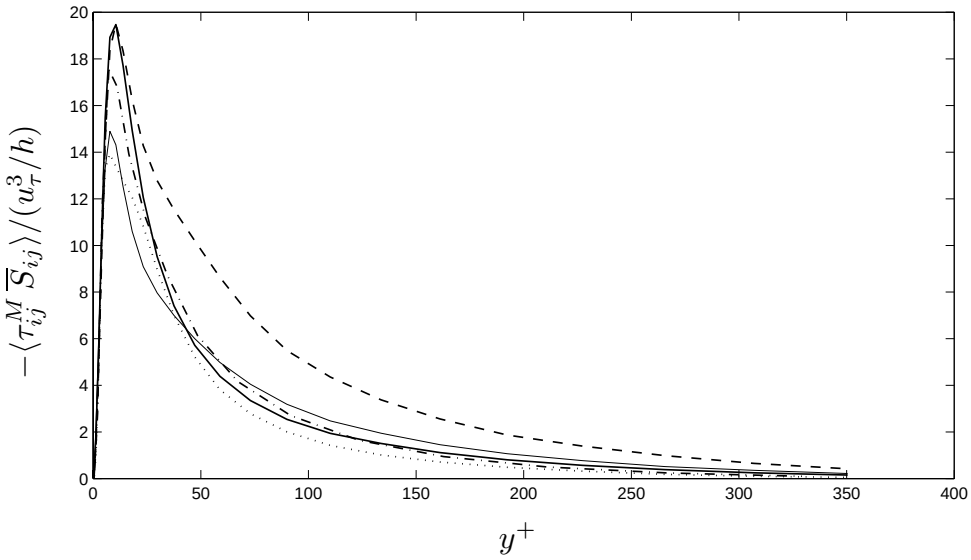

FIGURE 13. Mean model dissipation profile: Leonard model + dynamic Smagorinsky term, 48x49x48, Gaussian and top hat (Leonard: ——— , Smagorinsky: ———); dynamic Smagorinsky model, 48x49x48, Gaussian and top hat: – – – – ; dynamic Smagorinsky model, 32x33x32, sharp cutoff: —·— ; dynamic Smagorinsky model, 48x49x48, sharp cutoff: ····· .

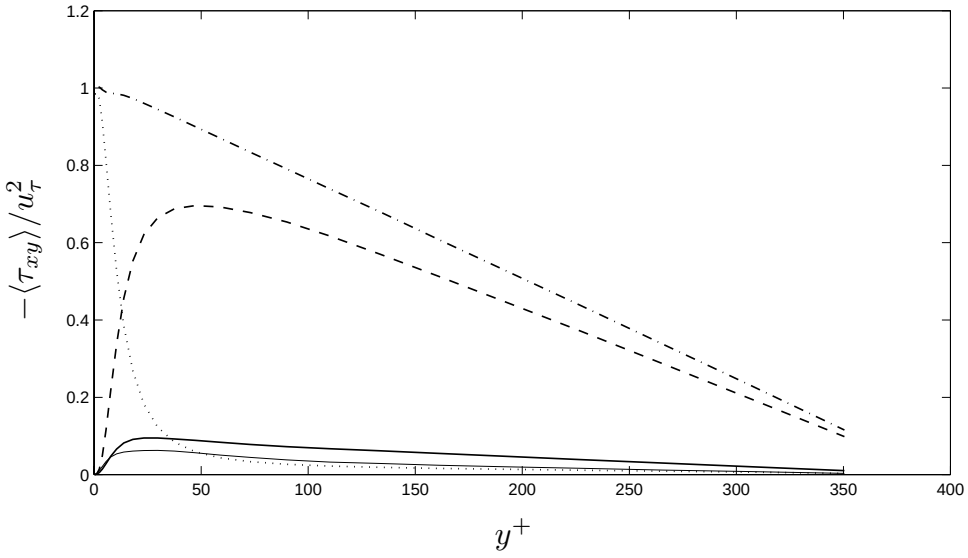

FIGURE 14. Mean stress profile for 48x49x48 LES using the Leonard model + dynamic Smagorinsky term, Gaussian and top hat: Leonard stress: ——, dynamic Smagorinsly stress: ——; Reynolds stress, $(\langle\overline{u}\rangle\langle\overline{v}\rangle - \langle\overline{u}\,\overline{v}\rangle)/u_\tau^2$: - - - - ; viscous stress, $2\nu\langle\overline{S}_{xy}\rangle/u_\tau^2$: ····· ; total stress: —·— .

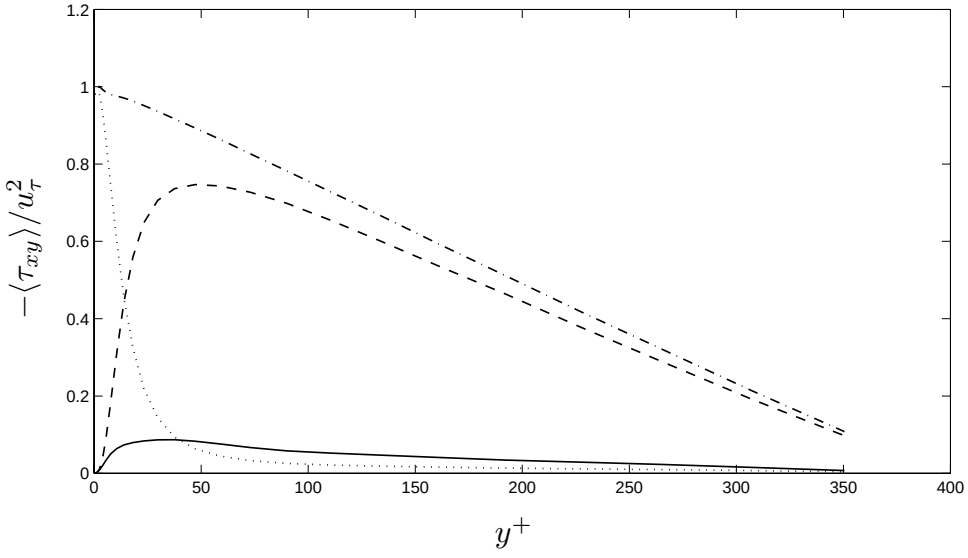

FIGURE 15. Mean stress profile for 48x49x48 LES using the dynamic Smagorinky model, Gaussian and top hat: model stress: ——; Reynolds stress, $(\langle\overline{u}\rangle\langle\overline{v}\rangle - \langle\overline{u}\,\overline{v}\rangle)/u_\tau^2$: - - - - ; viscous stress, $2\nu\langle\overline{S}_{xy}\rangle/u_\tau^2$: ····· ; total stress: —·— .

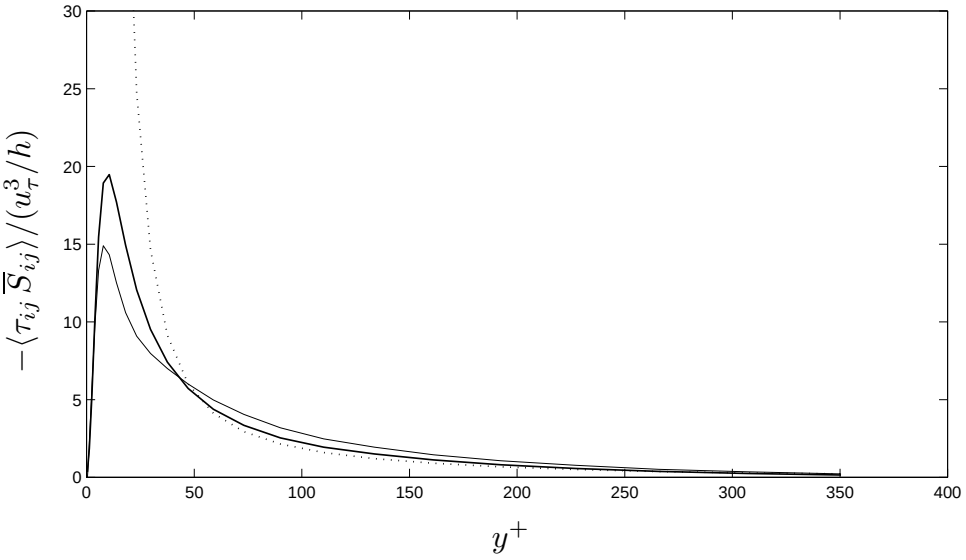

FIGURE 16. Mean dissipation profile for 48x49x48 LES using the Leonard model + dynamic Smagorinsky term, Gaussian and top hat: Leonard dissipation: ——— ; dynamic Smagorinsly dissipation: ——— ; viscous dissipation, $2\nu\,\langle \overline{S}_{ij}\overline{S}_{ij}\rangle/(u_\tau^3/h)$: ····· .

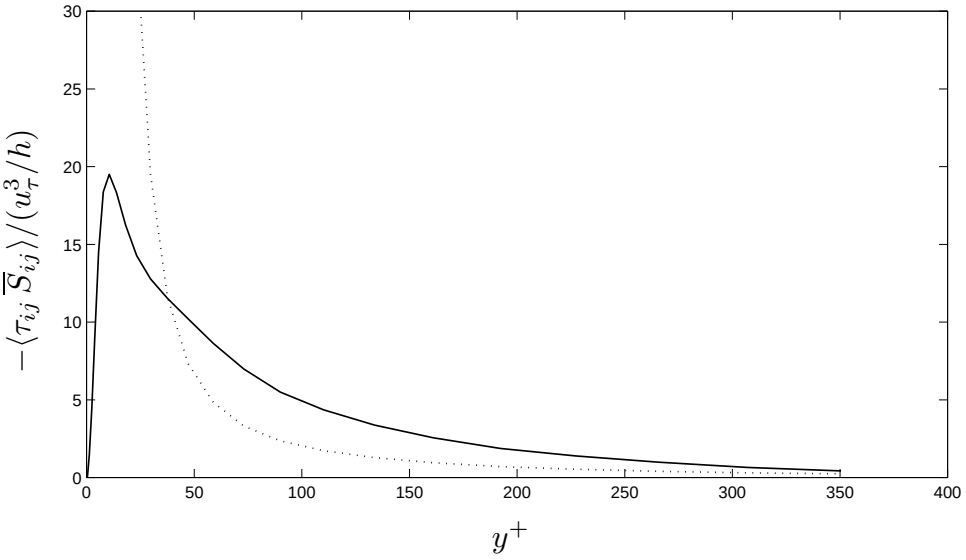

FIGURE 17. Mean dissipation profile for 48x49x48 LES using the dynamic Smagorinsky model, Gaussian and top hat: model dissipation: ——— ; viscous dissipation, $2\nu\,\langle \overline{S}_{ij}\overline{S}_{ij}\rangle/(u_\tau^3/h)$: ····· .

4. Conclusions

A new mixed model which uses the one-term Leonard model supplemented by a purely dissipative dynamic Smagorinsky term has been developed and tested in LES of decaying homogeneous turbulence and of channel flow. The dynamic procedure has been used to determine the coefficient of the Smagorinsky term. The one-term Leonard model provides for significant local backscatter while remaining globally dissipative. In *a priori* testing, its correlation with DNS was greater than 0.9. However, this model was found to provide too little dissipation in actual LES although it didn't blow up. Hence the need for the added dissipation provided by the dynamic Smagorinsky term in the mixed model. In 64^3 LES of decaying homogeneous turbulence started from Gaussian filtered 256^3 DNS at $Re_\lambda \simeq 90$, the new mixed dynamic model performed significantly better than the dynamic Smagorinsky model with same filtering; it also outperformed the dynamic Smagorinsky model with sharp cutoff filtering: much better energy spectra, energy decay, and enstrophy decay. For the preliminary 48^3 LES runs on the channel flow at $Re_\tau = 395$, the LES filter was Gaussian in the homogeneous directions and top hat in the non-homogeneous direction. The mixed dynamic model also outperformed the dynamic Smagorinsky model in that case. However, the dynamic Smagorinsky model with sharp cutoff test filtering in the homogeneous directions and no test filtering in the non-homogeneous direction still produced a better mean velocity profile. This result calls for further investigations.

REFERENCES

Bardina, J., Ferziger, J. H. & Reynolds, W. C. 1983 Improved turbulence models based on large eddy simulation of homogeneous incompressible turbulence. *Report TF-19*, Thermosciences Div., Dept. of Mech. Eng., Stanford University.

Borue, V. & Orszag, A. 1998 Local energy flux and subgrid-scale statistics in three-dimensional turbulence. *J. Fluid Mech.* **366,** 1-31.

Carati, D., Ghosal, S. & Moin, P. 1995 On the representation of backscatter in dynamic localization models. *Phys. Fluids.* **7**(3)**,** 606-616.

Carati, D., Jansen, K. & Lund, T. 1995 A family of dynamic models for large-eddy simulation. *Annual Research Briefs*, Center for Turbulence Research, NASA Ames/Stanford Univ., 35-40.

Carati, D. & Cabot, W. 1996 Anisotropic eddy viscosity models. *Proc. Summer Program*, Center for Turbulence Research, NASA Ames/Stanford Univ., 249-258.

Carati, D.& Vanden Eijnden, E. 1997 On the self-similarity assumption in dynamic models for large eddy simulations. *Phys. Fluids.* **9**(7)**,** 2165-2167 (L).

Carati, D., Winckelmans, G. S. & Jeanmart, H. 1998 On reversibility in modeling for large eddy simulations. (In preparation.)

Clark, R. A., Ferziger, J. H. & Reynolds, W. C. 1979 Evaluation of subgrid-scale models using an accurately simulated turbulent flow. *J. Fluid Mech.* **91,** 1-16.

Cottet, G.-H. 1996 Artificial viscosity models for vortex and particle methods. *J. Comput. Phys.* **127,** 299-308.

Cottet, G.-H. 1997 Anisotropic subgrid-scale numerical schemes for Large Eddy Simulations of turbulent flows. (Submitted Sept. 1997.)

Cottet, G.-H. & Wray, A. A. 1997 Anisotropic grid-based formulas for subgrid-scale models.*Annual Research Briefs*, Center for Turbulence Research, NASA Ames/Stanford Univ., 113-122.

Dantinne, G., Jeanmart, H., Winckelmans, G. S., Legat, V. & Carati, C. 1998 Hyper-viscosity and vorticity-based models for subgrid-scale modeling. *Applied Scientific Research.* **59,** 409-420.

Domaradzki, J. A. & Saiki, E. M. 1997 A subgrid-scale model based on the estimation of unresolved scales of turbulence. *Phys. Fluids.* **9,** 2148-2164.

Domaradzki, J. A. & Loh K.-C. 1998 The subgrid-scale estimation model in the physical space representation. submitted to Phys. Fluids.

Germano, M., Piomelli, U., Moin, P. & Cabot, W. 1991 A dynamic subgrid-scale eddy-viscosity model. *Phys. Fluids A.* **3**(7)**,** 1760-1765.

Ghosal, S., Lund, T. S. & Moin, P. 1992 A local dynamic model for large-eddy simulation. *Annual Research Briefs*, Center for Turbulence Research, NASA Ames/Stanford Univ., 3-25.

Ghosal, S., Lund, T. S., Moin, P. & Akselvoll, K. 1995 A dynamic localization model for large-eddy simulation of turbulent flows. *J. Fluid Mech.* **286,** 229-255.

Ghosal, S. & Moin, P. 1995 The basic equations for the large-eddy simulation of turbulent flows in complex geometry. *J. Comput. Phys.* **118,** 24-37.

Horiuti, K. 1997 A new dynamic two-parameter mixed model for large-eddy simulation. *Phys. Fluid.* **9**(11)**,** 3443-3464.

Leonard, A. 1974 Energy cascade in large-eddy simulations of turbulent fluid flows. *Adv. Geophys.* **18,** 237.

Leonard, A. 1997 Large-eddy simulation of chaotic convection and beyond. *AIAA Paper 97-0204, 35th Aerospaces Sciences Meeting & Exhibit*, Jan. 6-10, 1997, Reno, N.,

Liu, S., Meneveau, C. & Katz, J. 1994 On the properties of similarity subgrid-scale models as deduced from measurements in a turbulent jet. *J. Fluid Mech.* **275,** 83-119.

Lund, T. S. & Novikov, E. A. 1992 Parametrization of subgrid-scale stress by the velocity gradient tensor. *Annual Research Briefs*, Center for Turbulence Research, NASA Ames/Stanford Univ., 27-43.

Mansour, N. N., Moser, R. D. & Kim, J. 1996 Reynolds number effects in low Reynolds number turbulent channels. (In preparation, data in AGARD database)

McMillan, O. J. & Ferziger, J. H. 1979 Direct testing of subgrid-scale models. *AIAA J.* **17,** 1340.

Moin, P., Carati, D., Lund, T., Ghosal, S, & Akselvoll, K. 1994 Developments and applications of dynamic models for large eddy simulation of complex flows. *AGARD-CP-551, 74th Fluid Dynamics Symposium on Application of Direct and Large Eddy Simulation to Transition and Turbulence*, Chania, Crete, Greece, 1: 1-9.

Piomelli, U., Moin, P. & Ferziger, J. H. 1988 Model consistency in large eddy simulation of turbulent channel flows. *Phys. Fluids.* **31**(7)**,** 1884-1891.

Rodi, W. & Mansour, N. N. 1993 Low-Reynolds-number $\kappa - \epsilon$ modeling with the aid of direct simulation data. *J. Fluid Mech.* **250,** 509-529.

Salvetti, M. V. & Banerjee, S. 1995 *A priori* tests of a new dynamic subgrid-scale model for finite-difference large-eddy simulations. *Phys. Fluids.* **7**(11)**,** 2831-2847.

Smagorinsky, J. 1963 General circulation experiments with the primitive equations. *Mon. Weather Rev.* **91,** 99-164.

Winckelmans, G. S., Lund, T. S., Carati, D. & Wray, A. A. 1996 *A priori* testing of subgrid-scale models in the velocity-pressure and the vorticity-velocity formulations, *Proc. Summer Program*, Center for Turbulence Research, NASA Ames/Stanford Univ., 309-328.

Zang, Y., Street, R. L. & Koseff, J. 1993 A dynamic mixed subgrid-scale model and its application to turbulent reciculating flows. *Phys. Fluids A.* **5,** 3186.